sive or deficient products on target N/Z is seen to be strong and markedly different from that of the isobaric cross section. This point illustrates the danger of drawing conclusions about the dependence of isobaric yields on target A or N/Z from measurements on single isobars.

V. CONCLUSIONS

The present investigation of the isobaric yield distribution at $A=66$–74 resulting from spallation of 3 targets with $A=96$ by 1.8 GeV protons reveals the dependence of this distribution on the N/Z value of the target. A change of 4 charge units for the targets thus results in a concomitant change in Z_p at $A=72$ of 0.6 units. This shift in turn results in order of magnitude differences in isobaric yield ratios obtained for the different targets. These conclusions indicate that while the hypothesis of invariant isobaric yield ratios[6] for spallation reactions may hold true in a comparison of targets with similar N/Z values, it is not generally valid. The correlation with N/Z is further confirmed in the comparison of the present results with those of Kaufman[4] and is also in agreement with cascade-evaporation calculations. It is of interest to note that the correlation of the Z_p values, isobaric yield ratios, and cross sections of very neutron deficient or excessive products with target N/Z is only weakly affected by the obvious differences in the reaction mechanism for the various targets studied by Kaufman[4] and by us. It would be of interest to perform measurements of this type in other mass regions in order to test the generality of these notions.

ACKNOWLEDGMENTS

The cooperation of the operating staff of the Cosmotron is appreciated. The chemical yield measurements were ably performed by Dr. R. W. Stoenner, Dr. J. K. Rowley, and members of the analytical chemistry group. Special thanks are due to Dr. S. Kaufman for making the results of his counter efficiency measurements available to the authors. The results of the Monte Carlo cascade calculations were kindly made available by Dr. G. Friedlander. We wish to thank Dr. S. Katcoff for a critical reading of the manuscript.

PHYSICAL REVIEW VOLUME 133, NUMBER 2B 27 JANUARY 1964

Elastic Scattering of Protons by Fe^{56}, Fe^{58}, and Ni^{58} at 10.9 and 11.7 MeV

J. BENVENISTE AND A. C. MITCHELL
Lawrence Radiation Laboratory, University of California, Livermore, California

AND

C. B. FULMER
Oak Ridge National Laboratory, Oak Ridge, Tennessee*

(Received 5 August 1963)

Differential cross sections for elastic scattering of protons from Fe^{56}, Fe^{58}, and Ni^{58} were measured and compared. Differences in positions of the maxima and minima are observed; when compared with the results of extensive optical model analyses of other data these are shown to be consistent with a nuclear symmetry dependence of the real nuclear-potential well depth. A comparison of the $A=58$ data with previously reported $A=64$ data shows the positions of maxima and minima in the differential elastic-scattering cross sections to be much more sensitive to differences of $(N-Z)/A$ than to differences in nuclear deformation.

INTRODUCTION

THEORETICAL studies[1] have shown that there are reasons to expect a dependence of the real nuclear potential well depth V on the nuclear symmetry parameter $(N-Z)/A$;

$$V=V_0\pm[(N-Z)/A]V_1 \quad (1)$$

for protons and neutrons, respectively. In a recent optical model analysis of proton elastic scattering in the range of 9 to 22 MeV[2] the observed increase of the real well depth as a function of mass number was explained in part by a nuclear symmetry term in the potential. Optical model analyses of proton-nucleus elastic-scattering data[3,4] have shown that maxima and minima in elastic-scattering angular distributions occur at angular positions that are determined mainly by VR^n, where R is the nuclear radius and n increases with proton energy. It thus seems that the experimental study of proton-nucleus elastic scattering by isobars should be one of the most direct ways to obtain experimental information about the role of the nuclear symmetry parameter in elastic scattering and hence the effect it has on the real

* Operated for the U. S. Atomic Energy Commission by Union Carbide Corporation.

[1] A. M. Lane, Phys. Rev. Letters **8**, 171 (1962); an extensive bibliography is given in Ref. 5.

[2] F. G. Perey, Phys. Rev. **131**, 745 (1963).

[3] A. E. Glassgold, W. B. Cheston, M. L. Stein, S. B. Schuldt, and G. W. Erickson, Phys. Rev. **106**, 1207 (1957).

[4] A. E. Glassgold and P. J. Kellog, Phys. Rev. **107**, 1372 (1957).

nuclear potential. This was the principal motivation for the work reported here.

In a previous paper[5] the results of proton-nucleus elastic-scattering experiments with Ni^{64} and Zn^{64} targets were reported. In those experiments, at bombarding energies of 9.6 and 11.7 MeV, it was observed that the maxima and minima of the angular distributions for Ni^{64} occur at angles $\sim 4°$ smaller than the corresponding features of the Zn^{64} angular distributions. This shift was shown to be consistent with the presence of a nuclear symmetry term in the real nuclear potential. The isobaric targets have the same nuclear radius (at least the same value of $A^{1/3}$), and hence the effect of R in the VR^n term is removed. It is believed, however, that nuclei in this mass region can be easily set into oscillation, as is evidenced by Coulomb excitation data and the energy of the first 2+ level, and that this vibrational character, denoted by a root-mean-square (rms) deformation, is reflected in the elastic scattering.[6] It might be supposed that the shift observed in the elastic scattering angular distribution is more a product of the rms nuclear deformation parameter than of the nuclear symmetry parameter. Therefore, we decided to extend the investigation. In the previously reported $A=64$ case Ni^{64} has the larger $(N-Z)$ and the smaller rms deformation. Therefore, for the present investigation we selected the $A=58$ isobars wherein Fe^{58} has the larger $(N-Z)$ and the larger rms deformation parameter. If there were an appreciable influence of nuclear deformation on the positions of the maxima and minima of the elastic scattering angular distributions, a comparison of the data obtained in these two experimental investigations should give evidence of the effect.

EXPERIMENTAL

These experiments were performed with the external proton beam of the variable-energy cyclotron of the Lawrence Radiation Laboratory at Livermore. Detailed descriptions of the experimental arrangement are given in Ref. 5. A brief description is given here.

Upon emerging from the cyclotron the proton beam is magnetically analyzed, focused, and collimated to a diameter of $\frac{1}{8}$ in. Then after traversing a 40-in.-diam scattering chamber, it is collected in a Faraday cup which monitors the beam intensity. At the center of the scattering chamber is an eight-position target changer that is remotely controlled. Within the scattering chamber is a rotatable table with provisions for precisely mounting a detector such that the detector angle is remotely controlled and indicated in the control room, with a precision of ± 0.1 deg.

A thin foil placed in the path of the main beam serves to scatter protons 30° through a variable absorber into a double proportional counter. An anticoincidence circuit is used to make a differential range measurement of the beam with a precision of about 1%.

Back of the proportional counters is a scintillation counter. After the particle range has been measured, the absorber is reduced enough to allow about 1.5 MeV of proton energy to be deposited in the scintillation crystal. Pulses from the photomultiplier tube are fed into a "continuous-energy-monitor" (cem), a circuit which measures the average pulse height of the input pulses and yields a continuously visible meter reading. During the course of collecting data the cem reading was maintained constant within an increment corresponding to 0.1% of the beam energy; if the meter reading drifted outside this interval data collection was interrupted until the beam energy was corrected by the cyclotron operator.

The targets consisted of self supporting foils. The Fe^{58} foil was prepared by Robert Seegmiller of Los Alamos Scientific Laboratory from material enriched in Fe^{58} by the Isotopes Division of Oak Ridge National Laboratory. The Ni^{58} foil was prepared by E. B. Olzewski of ORNL. The isotopic assay of each of the foils, as given by the Isotopes Division of ORNL, is as follows:

Fe^{58} target	Fe^{54}	Fe^{56}	Fe^{57}	Fe^{58}	
	0.9%	18.7%	2.0%	78.4%	
Ni^{58} target	Ni^{58}	Ni^{60}	Ni^{61}	Ni^{62}	Ni^{64}
	99.25%	0.75%	<0.01%	<0.01%	<0.01%

An area survey of the surface density of the targets was made with "Verni-Ray,[7]" a device which measures the energy loss of alpha particles from a radioactive source. This revealed rather large nonuniformities which rendered gravimetric determinations of average surface density unreliable. Therefore, the target thickness was measured in the region where the beam struck by comparing Verni-Ray readings with those for a carefully weighed, uniform foil of the natural elements. In spite of these precautions, an unsuspected malfunction of the target changer during the 10.9-MeV run rendered imprecise our knowledge of where the beam actually struck the target. Subsequent analysis showed that this contributed an uncertainty to the measured differential cross sections of 3% for the Ni^{58} and 5% for the Fe^{58} data. This problem did not exist for the 11.7-MeV run and the assigned precision reflects the higher reliability of the data. For the forward angles ($<90°$), data were obtained with the normal to the target foil bisecting the scattering angle. Beyond 90° the plane of the scattering foil bisected the scattering angle.

Scattered particles from the targets were detected by a counter telescope consisting of a silicon p-n junction diode preceded by a gas proportional counter with offset center wire. Pulses from the gas proportional counter (dE/dx pulses) and from the silicon counter (E pulses)

[5] J. Benveniste, A. C. Mitchell, and C. B. Fulmer, Phys. Rev. **129**, 2173 (1963).
[6] B. Buck, Phys. Rev. **130**, 712 (1963).
[7] J. Benveniste, A. C. Mitchell, C. Shrader, and J. Zenger, Rev. Sci. Instr. **32**, 927 (1961).

TABLE I. Differential cross section for elastic scattering of protons. For Fe^{56} and Fe^{58} $E_p = 10.93$ MeV: For Ni^{58} $E_p = 10.88$ MeV.

	Fe^{56}		Fe^{58}		Ni^{58}	
$\theta_{c.m.}$ (deg)	$\sigma(\theta)$ (mb/sr)	± %	$\sigma(\theta)$ (mb/sr)	± %	$\sigma(\theta)$ (mb/sr)	± %
30.5	1.28×10^3	5	1.26×10^3	7	1.57×10^3	5
35.6	765	5	762	7	936	5
40.6	514	5	470	6	639	4
50.8	192	5	150	6	248	4
60.9	57.5	5	43.2	6	75.7	4
65.9	26.8	5	20.7	6	37.7	4
70.9	17.4	5	15.2	7	22.3	4
76.0	10.5	5	14.3	7	13.8	5
81.0	11.7	5	17.9	6	14.8	4
86.0	13.4	5	19.2	6	16.6	4
91.0	16.0	5	19.3	6	20.6	4
96.0	16.7	5	18.3	7	22.7	4
101.0	18.0	5	17.1	7	25.0	4
105.9	16.3	5	14.7	7	25.3	4
110.9	15.3	5	11.7	7	21.9	4
120.9	9.19	5	6.45	7	13.9	5
125.8	6.87	5	3.50	7	10.8	4
130.8	5.14	5	1.83	7	8.50	4
135.7	3.83	5	1.57	8	5.49	4
140.6	3.58	5	1.98	8	6.11	4
150.5	5.04	5	4.19	7	7.86	4
160.3	7.64	5	7.48	7	11.0	4
170.2	9.82	5	8.78	7	14.0	4

are fed into a multiplier network; output pulses of the latter identify detected particles as protons, deuterons, or alpha particles. Multiplier pulses due to protons were selected by a single-channel pulse-height analyzer and used to gate a multichannel analyzer which recorded the proton spectra. The silicon counter used for these experiments was thick enough to stop 11.5-MeV protons. For the 10.9-MeV run, this detector was used in the normal fashion; however, at 11.7 MeV, to avoid "fold over" of the elastic peak and consequent problems in identifying all the elastic events, the detector was used in the "slant"[8] condition—with the incident particles making an angle of 30° with the front surface.

TABLE II. Differential cross sections for proton elastic scattering at 11.7 MeV.

	Fe^{56}		Fe^{58}		Ni^{58}	
$\theta_{c.m.}$ (deg)	$\sigma(\theta)$ (mb/sr)	± %	$\sigma(\theta)$ (mb/sr)	± %	$\sigma(\theta)$ (mb/sr)	± %
20.5	4456	2	4308	2	5405	2
25.5	1973	2	2018	2	2326	2
30.6	1151	2	1145	2	1312	2
35.6	725	2	689	2	823	2
40.7	442	2	413	2	529	2
45.7	279	2	238	2	323	2
50.8	165	2	128	2	197	2
60.9	50.4	2	37.2	2	62.5	2
65.9	27.1	2	20.9	2	32.7	2
70.9	14.5	2	13.7	2.2	18.1	2.2
75.9	10.7	2.2	12.8	2.2	12.4	2.2
80.9	11.2	2	15.0	2.2	12.0	2.2
85.9	13.8	2	17.5	2	14.4	2.2
90.9	16.3	2	17.9	2	17.3	2
95.9	19.0	2	16.6	2	21.1	2
100.9	19.0	2	14.8	2	22.8	2
105.8	17.6	2	12.6	2	21.9	2
110.8	14.7	2.2	9.54	2.2	19.6	2
115.8	11.7	2.2	6.58	2.3	16.7	2
120.7	8.27	2.2	4.15	2.4	13.1	2.2
130.5	3.26	2.3	1.52	3.2	6.59	2.2
135.5	2.37	2.4	1.34	3.2	4.51	2.2
140.4	2.41	2.4	1.77	3.2	4.50	2.2
144.8	3.66	2.3	3.11	2.2	5.22	2.2
150.2	5.44	2.2	4.70	2.3	7.70	2.2
160.0	9.40	2.2	7.78	2.2	14.4	2
169.8	12.4	2.2	9.89	2.2	20.5	2

[8] J. Benveniste, R. Booth, A. C. Mitchell, Nucl. Instr. Methods 12, 67 (1961).

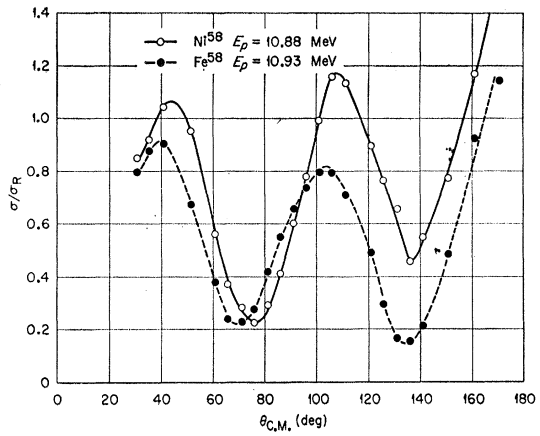

FIG. 1. Elastic scattering angular distributions for Fe^{58} and Ni^{58} at 10.9 MeV, plotted as ratio to Rutherford.

The two $A = 58$ target foils were mounted in adjacent positions on the target changer and observations of the two were made successively at each detection angle. In addition, a spectrum from a Mylar target was obtained at each angle; these spectra were compared with those from the metallic foils to obtain information about the carbon and oxygen impurities in the latter. This made it possible to correct the elastic scattering data at forward angles for contributions from the oxygen and carbon impurities. The Mylar data were especially useful when cross sections for inelastic scattering to first excited states[9] were determined. Data were also taken with a natural iron target (91.66% Fe^{56}) to obtain the elastic scattering angular distribution of Fe^{56} and to permit correcting the Fe^{58} data for the Fe^{56} impurity.

Successive data points were usually taken at 20° intervals. After two sweeps in which the detector angles were interleaved data were available for 10° steps from 30 to 170°. Additional observations were made in those angular regions where good definition of the differential cross sections was required.

RESULTS AND DISCUSSION

The results of the elastic scattering measurements are presented in Tables I and II. The values of the incident proton energy E are calculated for the beam after it passes through half the target thickness, hence the values are not the same for all targets in Table I. The Ni^{58} foil was ~5 mg/cm² thick while the iron foils were ~1.3 mg/cm² thick. Prior to obtaining the data in Table II the Ni^{58} foil was rolled to a thickness of ~1.5 mg/cm². Corrections were made for target impurities and (in the case of Fe^{58}) for the presence of appreciable amounts of other isotopes. The errors shown in Tables I and II include contributions from statistics, beam current integrator measurements, and geometric factors, in addition to those due to the target foil nonuniformities discussed above.

[9] J. Benveniste, A. C. Mitchell, B. Buck, and C. B. Fulmer, Phys. Rev. 133, B323 (1964), following paper.

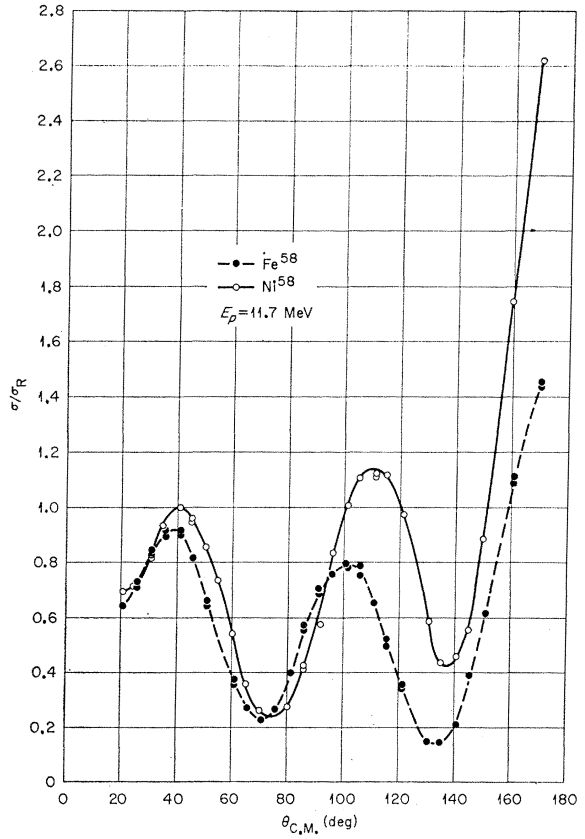

FIG. 2. Elastic scattering angular distributions for Fe^{58} and Ni^{58} at 11.7 MeV, plotted as ratio to Rutherford.

Figure 1 is a graphical presentation of the 10.9-MeV Fe^{58} and Ni^{58} data plotted as the ratios of the elastic scattering to Rutherford cross sections. A similar presentation of 11.7-MeV data for Fe^{58} and Ni^{58} is shown in Fig. 2. The 11.7-MeV data were repeated throughout the angular range, and the data points for both experimental runs are shown where they differ enough to be plotted separately. One obvious feature of the data as displayed in Fig. 1 and 2 is that the Ni^{58} cross sections, relative to those of Fe^{58}, are rather large at angles >100 deg. The 10.9-MeV Ni^{58} data presented here, are in good agreement, however, with the Ni^{58} data previously obtained at 10.7 MeV.[10]

The (p,n) threshold for Fe^{58} is 3.1 MeV and for Ni^{58} it is 9.3 MeV. Therefore, one would expect large compound elastic contributions to the Ni^{58} data and insignificantly small contributions to the Fe^{58} data. This phenomenon is apparent in Figs. 1 and 2. The effect of compound elastic scattering on the measured cross sections is more noticeable at large angles where the shape elastic scattering cross sections are small. This is consistent with the increase of the ordinates of the Ni^{58} data relative to the Fe^{58} data for angles >100 deg in Figs. 1 and 2. Similar but less pronounced contributions to the Zn^{64} data have been observed[5] at 9.6-MeV incident proton energy.

In principle, the compound elastic scattering cross sections can be calculated by the method used by Hauser and Feshbach.[11] This calculation, however, requires knowledge of the spins and parity of all available exit channels for protons and neutrons.[12] These data are not all available for the case of 10.9- and 11.7-MeV protons on Ni^{58}. An estimate of the compound elastic contribution to the measured angular distribution for Ni^{58} at 10.9 MeV was made by assuming it to be isotopic and plotting the ratio of elastic scattering to Rutherford cross sections with the measured elastic scattering data reduced by 1, 2, 3, 4, and 5 mb/sr. The resulting curves are shown in Fig. 3. Since the shape elastic scattering is small at large angles this should be the most sensitive region for estimating the compound elastic contribution to the measured cross sections. In Fig. 1 the value of σ/σ_R for Fe^{58} is smaller at the minimum near 135 deg than

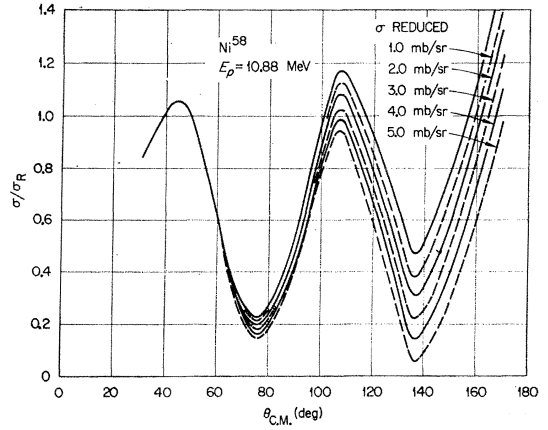

FIG. 3. Elastic scattering angular distribution for Ni^{58} at 10.9 MeV, plotted as ratio to Rutherford with the experimental cross sections reduced 1, 2, 3, 4, and 5 mb/sr.

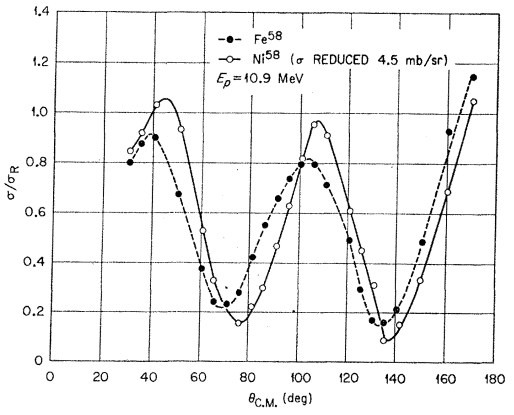

FIG. 4. 10.9-MeV σ/σ_R angular distributions for Fe^{58} and Ni^{58}, with estimated compound elastic correction.

[10] S. Kobayashi, K. Matsuda, Y. Nagahara, Y. Oda, and N. Yamamuro, J. Phys. Soc. Japan **15**, 1151 (1960).
[11] W. Hauser and H. Feshbach, Phys. Rev. **87**, 366 (1952).
[12] F. G. Perey (private communication).

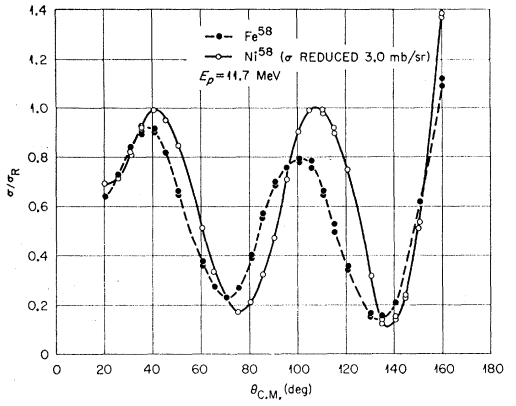

FIG. 5. 11.7-MeV σ/σ_R angular distributions for Fe^{58} and Ni^{58}, with estimated compound elastic correction.

at the minimum near 70 deg. If it is assumed that the shape elastic scattering of Ni^{58} should exhibit a similar feature the curves shown in Fig. 3 indicate that a reduction of the measured Ni^{58} cross sections by between 4 and 5 mb/sr is the proper correction to remove the contribution of compound elastic scattering in the region of the second minimum. It is expected that the compound elastic scattering is not isotropic but rather has an angular distribution of the form $A+B\cos^2\theta$. The anisotropy defined as $\sigma(0 \text{ deg})/\sigma(90 \text{ deg})$ is expected to be less than 2 however. Figure 4 is a comparison of the 10.9 MeV Fe^{58} and Ni^{58} data reduced by 4.5 mb/sr. In the same manner the compound elastic contribution to the Ni^{58} data at 11.7 MeV is estimated to be $\sim$3.0 mb/sr. Figure 5 is a comparison of the 11.7-MeV Fe^{58} and Ni^{58} data with the Ni^{58} data reduced by 3.0 mb/sr.

The most important result of the work reported here is that the maxima and minima of the Fe^{58} angular distributions (Figs. 1, 2, 4, and 5) occur at smaller angles than the corresponding features of the Ni^{58} angular distribution. This is consistent with a larger value of the real nuclear potential well depth for the isobar with the larger nuclear symmetry parameter. Similar results were obtained for Ni^{64} and Zn^{64} proton elastic scattering at 9.6 and 11.7 MeV.[5] Figure 6 is a comparison of proton elastic scattering angular distributions of the $A=64$ isobars at 11.7 MeV. This figure was published in Ref. 5 but is also included here for comparison.

In the $A=64$ case the isobar with the larger value of $(N-Z)$ has the smaller nuclear deformation parameter. In the $A=58$ case the isobar with the large value of $(N-Z)$ has the larger deformation parameter. In both cases the isobars with the larger values of $(N-Z)$ exhibit maxima and minima in the elastic scattering angular distributions that occur at smaller angles than the corresponding features of the angular distributions observed for the other isobars. These indicate that the positions of maxima and minima depend much more strongly on $(N-Z)$ than on nuclear deformation;

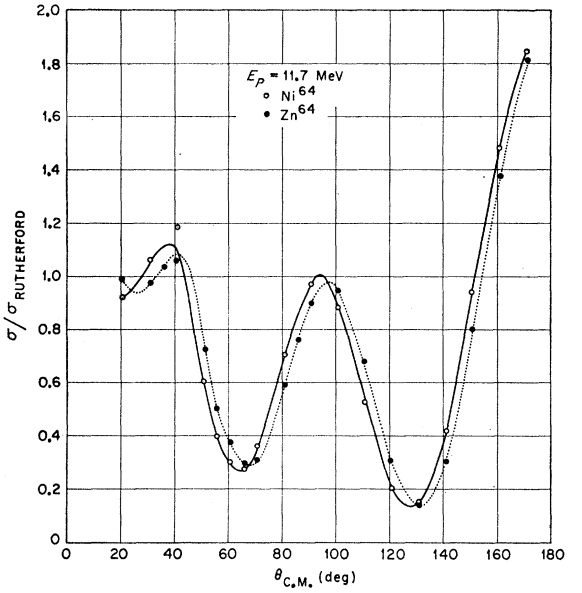

FIG. 6. Elastic scattering angular distributions for Ni^{64} and Zn^{64} at 11.7 MeV, plotted as ratio to Rutherford. These data are repeated from Ref. 5 for comparison with the $A=58$ data.

hence, the real nuclear potential well depth is determined in part by the nuclear symmetry parameter.

Further evidence of the effect of the nuclear symmetry parameter on proton-nucleus elastic scattering can be had by comparing the $A=58$ data with that obtained from Fe^{56}. The value of $(N-Z)$ for Fe^{56} is 4, for Fe^{58} it is 6, and for Ni^{58} it is 2; the values of A are almost the same for the three cases.

The elastic scattering angular distributions of Fe^{56} and Fe^{58} are compared in Fig. 7. Fe^{58} has both the larger

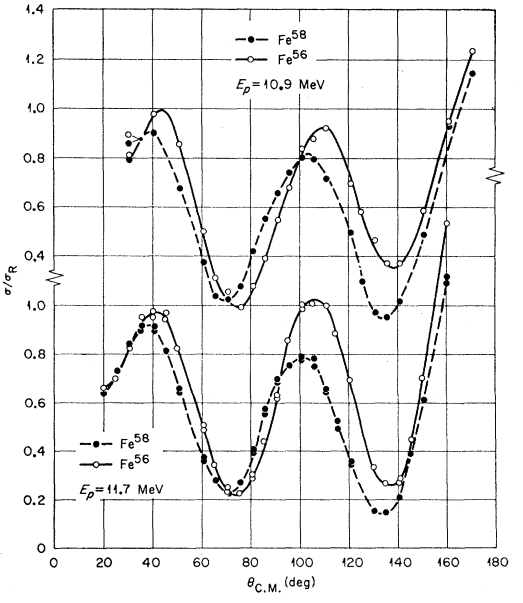

FIG. 7. Elastic scattering angular distributions for Fe^{56} and Fe^{58} at 10.9 and 11.7 MeV, plotted as ratio to Rutherford.

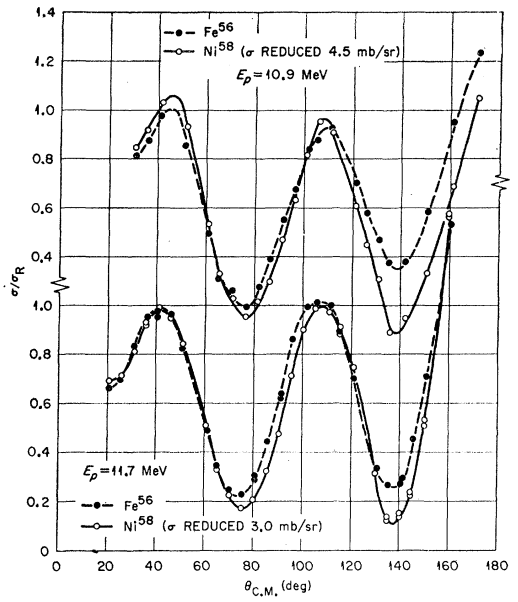

FIG. 8. Elastic scattering angular distributions of Fe^{56} and Ni^{58} at 10.9 MeV, and at 11.7 MeV, plotted as ratio to Rutherford. The Ni^{58} data has been corrected for the estimated compound elastic contribution.

value of $A^{1/3}$ and the larger nuclear symmetry parameter. The maxima and minima of the Fe^{58} angular distribution occur at smaller angles than the corresponding features of Fe^{56}.

The elastic scattering angular distributions of Fe^{56} and Ni^{58} are compared in Fig. 8. Fe^{56} has the larger nuclear symmetry parameter and Ni^{58} has the larger value of $A^{1/3}$; corresponding maxima and minima for the two targets occur at approximately the same angular positions. The results indicate that increasing the nuclear symmetry parameter has an effect on pronton-nucleus elastic scattering that is qualitatively the same as the effect of increasing the nuclear radius; they both shift the positions of maxima and minima to smaller angles. In Fig. 7 the effects add together, since Fe^{58} has both the larger $(N-Z)$ and the larger nuclear radius. In Fig. 8 the effects tend to cancel out, since Fe^{56} has the larger $(N-Z)$ and Ni^{58} has the larger nuclear radius. For the cases studied in the work reported here, increasing A from 56 to 58 has the same effect on the elastic scattering angular distribution as increasing $(N-Z)$ by 2.

Two additional features of the elastic scattering data reported here and in Ref. 5 are observed. These will be discussed briefly:

In both the $A=58$ and the $A=64$ cases of proton elastic scattering by isobars the targets with the larger deformation, i.e., Fe^{58} and Zn^{64} exhibit smaller amplitudes of the oscillations in the angular distributions than the other isobars. From Coulomb excitation data Fe^{56} is more deformable than Ni^{58} and slightly less deformable than Fe^{58}. The amplitudes of the oscillations of the Fe^{56} angular distribution are smaller than those for Ni^{58} and larger than those for Fe^{58}. These results are consistent with larger values of W, the imaginary potential well depth which in the nuclear optical model accounts for the absorption of incident particles, describing the nuclei with larger rms deformation parameter. Optical model analyses of proton-nucleus elastic scattering data[3,4] showed the effect of increasing W to be a decrease of the amplitudes of the oscillations.

The other rather prominent feature of the data is the behavior of the angular distributions at large angles, i.e. $\gtrsim$150 deg. For angles forward of the minima near 135° the elastic scattering cross sections decrease as the bombarding energy is increased from 10.9 to 11.7 MeV; at angles back of 150° this decrease is not observed and for Ni^{58} and Fe^{56} the cross sections at 160° and 170° are substantially larger at 11.7 MeV than at 10.9 MeV. In all cases in the work reported here and in Ref. 5 the σ/σ_R values at 160° and 170° are larger for the higher energy data. Some increase in the measured cross sections at large angles can be attributed to the increase in the number of oscillations in the angular distributions as the bombarding energy is increased; thus the 170° data points for 11.7 MeV are nearer an angular distribution maxima than the 170° points for lower bombarding energies. Such changes in the data at large angles have been previously observed.[13,14]

It is unlikely, however, that the large increase of the elastic scattering cross section for Ni^{58} at 160° and 170°, as the bombarding energy is increased from 10.9 to 11.7 MeV, can be attributed entirely to another oscillation in the angular distribution. The contribution from compound elastic scattering decreases as the bombarding energy is increased. Thus it does not contribute to the increase of the Ni^{58} cross sections that we observe at 160° and 170°. The increase is most likely due to a size resonance near 11.7 MeV or a large contribution from spin-orbit potential. The data suggest that a more extensive study of elastic scattering at large angles with variable energy is needed.

ACKNOWLEDGMENTS

The authors gratefully acknowledge the discussions and comments of R. H. Bassel and R. M. Drisko on this work.

[13] J. Benveniste, R. Booth, and A. C. Mitchell, Phys. Rev. **123**, 1818 (1961).

[14] L. L. Lee, Jr., and J. P. Schiffer, Argonne National Laboratory Report, ANL-6666, 1962 (unpublished).